

B physics at CDF – the Beauty of hadron collisions

D. Tonelli^{a*}

^aFermilab,
P.O. Box 500, Batavia, IL, 60510, USA

The CDF experiment at the Tevatron $p\bar{p}$ collider established that extensive and detailed exploration of the b -quark dynamics is possible in hadron collisions, with results competitive and supplementary to those from e^+e^- colliders. This provides an unique, rich, and highly rewarding program that is currently reaching full maturity. I report a few recent world-leading results on rare decays, CP-violation in B_s^0 mixing, and $b \rightarrow s$ penguin decays.

1. Introduction

Precise results from the successful B -factories experiments disfavor large contributions from non standard model (SM) physics in tree-dominated bottom meson decays. Agreement with the SM within theory uncertainties is also manifest in higher-order processes, such as $K^0-\bar{K}^0$ or $B^0-\bar{B}^0$ flavor mixing. The emerging picture confirms the Cabibbo-Kobayashi-Maskawa (CKM) *ansatz* as the leading pattern of flavor dynamics. Non-SM contributions, if any, are small corrections, or appear well beyond the TeV scale (and the LHC reach), or have an unnatural, highly fine-tuned flavor structure that escaped all experimental tests to date. The last chances to avoid such a disappointing *impasse* include the physics of bottom-strange mesons, still fairly unexplored, along with a few rare B^0 decays, not fully probed at the B -factories because of limited event statistics.

The CDF experiment at the Tevatron is currently leading the exploration of this physics, owing to CP-symmetric initial states in $\sqrt{s} = 1.96$ TeV $p\bar{p}$ collisions, large event samples collected by a well-understood detector, and mature analysis techniques. CDF is a multipurpose magnetic spectrometer surrounded by 4π calorimeters and muon detectors. Most relevant for B physics are the tracking, particle-identification (PID) and muon detectors, and the trigger sys-

tem. Six layers of double-readout silicon microstrip detectors between 2.5 and 22 cm from the beam, and a single-readout layer at 1.5 cm radius, provide precise vertex reconstruction, with approximately 15 (70) μm resolution in the azimuthal (longitudinal) direction. A drift chamber provides 96 samplings of three-dimensional charged-particles trajectories between 40 and 140 cm radii in $|\eta| < 1$, for a transverse momentum resolution of $\sigma_{p_T}/p_T^2 = 0.1\%/(\text{GeV}/c)$. Specific ionization measurements in the chamber allow 1.5σ separation between charged kaons and pions, approximately constant at momenta larger than 2 GeV/ c . A comparable identification is achieved at lower momenta by an array of scintillator bars at 140 cm radius, which measure the time-of flight. Muons with $p_T > 1.5(2.2)$ GeV/ c are detected by planar drift chambers at $|\eta| < 0.6$ ($0.6 < |\eta| < 1.0$).

Low- p_T dimuon triggers select J/ψ , rare B , and bottomonia decays. They collected approximately 40 millions J/ψ decays in 5 fb^{-1} of data, used to reconstruct roughly 6,000 $B_s^0 \rightarrow J/\psi\phi$, 20,000 $B^0 \rightarrow J/\psi K^*(892)^0$, and 52,000 $B^+ \rightarrow J/\psi K^+$ decays. A trigger on charged particles displaced from the primary vertex collects hadronic heavy-flavor decays. It relies on dedicated custom electronics to reconstruct tracks in the silicon with offline-like (48 μm) impact parameter resolution, within 20 μs of the trigger latency. This yielded approximately 50 millions $D^0 \rightarrow K^-\pi^+$, 13,000 $B_s^0 \rightarrow D_s^-(\pi^+\pi^-)\pi^+$, and 12,000 $B^0 \rightarrow K^+\pi^-$ decays in 5 fb^{-1} of data.

*for the CDF Collaboration

CDF has currently collected 8 fb^{-1} of physics-quality data. The sample size will reach 10 fb^{-1} in October 2011. Additional 6 fb^{-1} will be collected if the proposed three-year extension will be funded.

In the following I report some recent, world-leading results, selected among those more sensitive to the presence of non-SM particles or couplings. Branching fractions indicate CP-averages, K^{*0} is shorthand for the $K^*(892)^0$ meson, and charge-conjugate decays are implied everywhere.

2. Polarization in $B_s^0 \rightarrow \phi\phi$ decays

The $B_s^0 \rightarrow \phi\phi$ decay proceeds through a penguin-dominated $b \rightarrow s\bar{s}s$ transition and was first detected by CDF a few years back. We recently improved the measurement of branching fraction using 295 ± 20 events reconstructed in 2.9 fb^{-1} of data collected by the displaced-track trigger. We obtain $\mathcal{B}(B_s^0 \rightarrow \phi\phi) = [2.40 \pm 0.21 \text{ (stat.)} \pm 0.27 \text{ (syst.)} \pm 0.82(\mathcal{B})] \times 10^{-5}$ [1]. The last uncertainty is due to the uncertainty on $\mathcal{B}(B_s^0 \rightarrow J/\psi\phi)$, used as a reference.

Three polarization amplitudes enrich the phenomenology of the $B_s^0 \rightarrow \phi\phi$ decay. They correspond to the allowed values of orbital angular momentum ($\ell = 0, 1, \text{ or } 2$) in the decay of a pseudo-scalar into two vector particles ($B \rightarrow VV$). A determination of these amplitudes may contribute useful insight into the puzzling picture of $B \rightarrow VV$ polarizations, where experimental data in $B^{0(+)} \rightarrow \phi K^{*(+)}$ decays disfavor first-order predictions of small transverse component ($f_T = \mathcal{O}(m_V^2/m_B^2) \approx 4\%$, where m are the masses), possibly suggesting contributions from non-SM amplitudes [2].

We report the first measurement of $B_s^0 \rightarrow \phi\phi$ polarization, using the sample employed for the branching fraction measurement [3]. We fit the mass of the four kaons and their angular distributions (in helicity basis). The angular acceptance, extracted from simulation, is validated by measuring the polarization of $B_s^0 \rightarrow J/\psi\phi$ decays to be consistent with results from an independent sample [4]. The small bias due to decay-length requirements in the trigger is included in the systematic uncertainties. In analogy with

measurements of similar $b \rightarrow s$ penguin decays, the results are at odds with naive theory predictions. We measure $|A_0|^2 = 0.348 \pm 0.041 \text{ (stat.)} \pm 0.021 \text{ (syst.)}$, $|A_{||}|^2 = 0.287 \pm 0.043 \text{ (stat.)} \pm 0.011 \text{ (syst.)}$, $|A_{\perp}|^2 = 0.365 \pm 0.044 \text{ (stat.)} \pm 0.027 \text{ (syst.)}$ for the polarization amplitudes, and $\cos(\delta_{||}) = -0.91_{-0.13}^{+0.15} \text{ (stat.)} \pm 0.09 \text{ (syst.)}$ for the phase difference between the $A_{||}$ and A_0 amplitudes. Further extensions of this analysis to larger samples will provide information on the decay-width difference $\Delta\Gamma$ in B_s^0 mesons.

3. Rare $B \rightarrow \mu^+\mu^-$ and $B \rightarrow h\mu^+\mu^-$ decays

Decays mediated by flavor changing neutral currents, such as $B_{(s)}^0 \rightarrow \mu^+\mu^-$ or $B \rightarrow h\mu^+\mu^-$ are highly suppressed in the SM because they occur only through higher order loop diagrams. Their phenomenology provide enhanced sensitivity to a broad class of non-SM contributions.

The $B_{(s)}^0 \rightarrow \mu^+\mu^-$ rate is proportional to the CKM matrix element $|V_{td}|^2(|V_{ts}|^2)$, and is further suppressed by helicity factors. The SM expectations for these branching fractions are $\mathcal{O}(10^{-9})$, ten times smaller than the current experimental sensitivity. An observation of these decays at the Tevatron would unambiguously indicate physics beyond the SM. Or, even improved exclusion-limits strongly constrain the available space of parameters of several SUSY models.

The latest CDF search for $B_{(s)}^0 \rightarrow \mu^+\mu^-$ decays uses 3.7 fb^{-1} of data collected by the dimuon trigger with $p_T(\mu) > 2 \text{ GeV}/c$ [5]. A loose preselection based on opposite-charge dimuon transverse momentum and muon identification criteria (quality of matching with track, energy deposit in the calorimeter, specific ionization energy loss), rejects combinatoric background and charmless B decays. Further rejection is achieved by selecting on the decay-length significance (λ/σ_λ) against prompt background and on the isolation of the $B_{(s)}^0$ meson candidate, to exploit the harder fragmentation of b -mesons with respect to light-quark background. In addition, we require the candidate to point back to the primary vertex to further reduce combinatoric background and partially reconstructed b -hadron decays. The resulting event sample contains about 55,000 can-

didates, mostly coming from combinatoric background. To further enhance purity we use an artificial neural network classifier (NN) that combines information from the above observables into a single scalar discriminating quantity. Signal distributions are modeled from detailed simulation; backgrounds from mass-sidebands in data. The signal rate is normalized to 20,000 $B^+ \rightarrow J/\psi(\rightarrow \mu^+\mu^-)K^+$ reconstructed in the same sample. The ratio of trigger acceptances between signal and normalization modes ($\simeq 25\%$) is derived from simulation, the relative trigger efficiencies ($\simeq 1$) are extracted from unbiased data and the relative offline-selection efficiency ($\simeq 80\%$) is determined from simulation and data. The expected average number of background events in the search region is obtained by extrapolating events from the mass-sidebands. The validity of this extrapolation is checked by comparing predicted and observed background yields in several independent control samples including like-sign dimuons, opposite-sign dimuons with negative decay-length, and opposite-sign dimuons with one muon failing the muon-quality requirements. Small contributions of punch-through hadrons from $B_{(s)}^0 \rightarrow h^+h'^-$ decays are included in the estimate of total background. We optimize the limit by combining three independent ranges for the NN discriminator (with efficiencies ranging from 44 to 12%) to obtain the *a priori* best expected 90% C.L. upper limit on $\mathcal{B}(B_{(s)}^0 \rightarrow \mu^+\mu^-)$ (see fig. 1). The resulting 90 (95)% CL upper limits are

$$\mathcal{B}(B_s^0 \rightarrow \mu^+\mu^-) < 3.6(4.3) \times 10^{-8}, \quad (1)$$

$$\mathcal{B}(B^0 \rightarrow \mu^+\mu^-) < 6.0(7.6) \times 10^{-9}. \quad (2)$$

These results are the most stringent currently available and reduce significantly the allowed parameter space for a broad range of SUSY models. An update of this analysis with approximately doubled sample size will further improve them soon.

We also updated the analysis of $B^0 \rightarrow K^{*0}(\rightarrow K^+\pi^-)\mu^+\mu^-$, $B^+ \rightarrow K^+\mu^+\mu^-$, and $B_s^0 \rightarrow \phi(\rightarrow K^+K^-)\mu^+\mu^-$ decays to 4.4 fb⁻¹ of data [6]. These are suppressed in the SM ($\mathcal{B} \approx 10^{-6}$), with amplitudes dominated by penguin and box

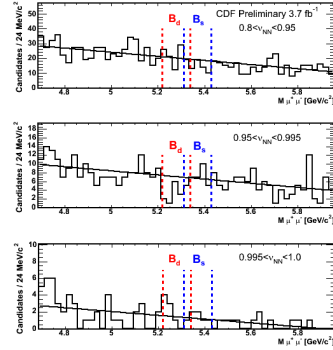


Figure 1. Distribution of $\mu^+\mu^-$ mass in three independent ranges of the NN classifier.

$b \rightarrow s$ transitions. Despite the presence of final-state hadrons, accurate predictions greatly sensitive to non-SM contributions are possible for relative quantities based on angular-distributions of final state particles. The B^+ and B^0 decays have been previously studied, while the B_s^0 channel has not been observed yet. We use a large sample of high-purity dimuon candidates combined in a common vertex with one or two charged particles, whose masses are assigned as appropriate for each final state. In the B^0 decay, the mass hypothesis yielding the $K\pi$ mass closer to the known K^{*0} mass is chosen, resulting in the proper assignment about 92% of the times. A NN that uses information from kinematics and particle-identification greatly improves signal-to-background discrimination. It is trained on simulated signals and mass-sideband data. The simulation is tuned to reproduce accurately the data using the corresponding resonant channels ($B \rightarrow J/\psi h$). The NN is optimized for maximum expected statistical resolution on the branching ratio and asymmetry measurements.

Prominent signals of $120 \pm 16 B^+ \rightarrow K^+\mu^+\mu^-$ and $101 \pm 12 B^0 \rightarrow K^{*0}\mu^+\mu^-$ events (fig. 2, left) are observed. The absolute branching fractions, measured using the resonant decays as a reference, are $[0.38 \pm 0.05 (stat.) \pm 0.03 (syst.)] \times 10^{-6}$ and $[1.06 \pm 0.14 (stat.) \pm 0.09 (syst.)] \times 10^{-6}$, respectively, consistent and competitive with pre-

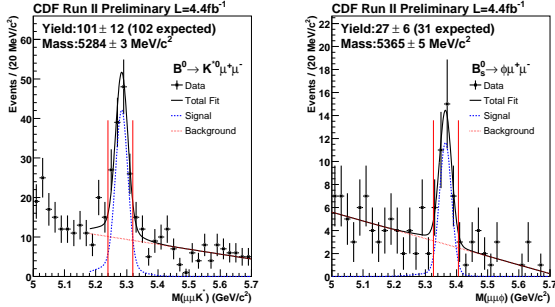


Figure 2. Distribution of $K^+\pi^-\mu^+\mu^-$ mass (left) and $K^+K^-\mu^+\mu^-$ (right).

vious determinations [2]. In addition, 27 ± 6 $B_s^0 \rightarrow \phi\mu^+\mu^-$ events are reconstructed, corresponding to the first observation of this decay, with a significance in excess of 6σ . The branching ratio, $(1.44 \pm 0.33 \text{ (stat.)} \pm 0.46 \text{ (syst.)}) \times 10^{-5}$, is consistent with theory predictions, and corresponds to the rarest B_s^0 decay ever observed to date. We use the B^+ and B^0 signals for the first measurement in hadron collisions of branching ratios, muon forward-backward asymmetry (A_{FB}), and K^{*0} longitudinal polarization, as a function of the dimuon mass. The asymmetry is greatly sensitive to non-SM particles and is determined from a fit to the $\cos(\theta_\mu)$ distributions, θ_μ being the helicity angle between the μ^+ (μ^-) and the opposite of the B (\bar{B}) direction in the dimuon rest frame. Angular acceptances are determined from simulation. Figure 3 shows the asymmetry as a function of dimuon mass. Integrated in the $1\text{--}6 \text{ GeV}^2/c^4$ range, where theory predictions are most reliable, it equals $A_{FB}(1 < q^2 < 6) = 0.43_{-0.37}^{+0.36} \text{ (stat.)} \pm 0.06 \text{ (syst.)}$, consistent with Belle and Babar determinations [2]. CDF plans to achieve world-leading results by summer 2011 with the anticipated 2–3 factors increase in statistics, due to additional data, triggers, and reconstructed final states.

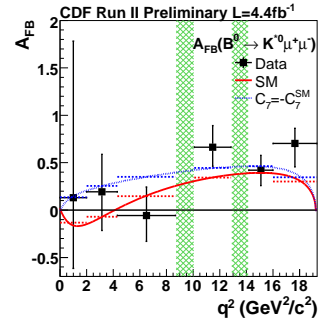


Figure 3. Forward-backward asymmetry in $B^0 \rightarrow K^{*0}\mu^+\mu^-$ as a function of dimuon mass.

4. Measurement of the B_s^0 mixing phase

Non-SM contributions have not yet been excluded in $B_s^0\text{--}\bar{B}_s^0$ mixing. Their magnitude is constrained to be small by the precise determination of the frequency [7]. However, knowledge of only the frequency leaves possible non-SM contributions to the (CP-violating) mixing phase unconstrained. The time evolution of flavor-tagged $B_s^0 \rightarrow J/\psi\phi$ decays allow a determination of this phase largely free from theory uncertainties. These decays probe the phase-difference between the mixing and the $\bar{b} \rightarrow \bar{c}c\bar{s}$ quark-level transition, $\beta_s^{J/\psi\phi} = \beta_s^{\text{SM}} + \beta_s^{\text{NP}}$, which equals $\beta_s^{\text{SM}} = \arg(-V_{ts}V_{tb}^*/V_{cs}V_{cb}^*) \approx 0.02$ in the SM and is extremely sensitive to non-SM physics in the mixing. A non-SM contribution (β_s^{NP}) would also enter $\phi_s^{J/\psi\phi} = \phi_s^{\text{SM}} - 2\beta_s^{\text{NP}}$, which is the phase difference between mixing and decay into final states common to B_s^0 and \bar{B}_s^0 , and is also tiny in the SM: $\phi_s^{\text{SM}} = \arg(-M_{12}/\Gamma_{12}) \approx 0.004$. Because the SM values for $\beta_s^{J/\psi\phi}$ and $\phi_s^{J/\psi\phi}$ cannot be resolved with the precision of current experiments, the following approximation is used: $\phi_s^{J/\psi\phi} \approx -2\beta_s^{\text{NP}} \approx -2\beta_s^{J/\psi\phi}$, which holds in case of sizable non-SM contributions. Note that the phase $\phi_s^{J/\psi\phi}$ also modifies the decay-width difference between light and heavy states, $\Delta\Gamma = \Gamma_L - \Gamma_H = 2|\Gamma_{12}|\cos(\phi_s^{J/\psi\phi})$, which enters in the $B_s^0 \rightarrow J/\psi\phi$ amplitude and equals

$\Delta\Gamma^{\text{SM}} \approx 2|\Gamma_{12}| = 0.086 \pm 0.025 \text{ ps}^{-1}$ in the SM [8].

We updated the measurement of the time-evolution of flavor-tagged $B_s^0 \rightarrow J/\psi(\rightarrow \mu^+\mu^-)\phi(\rightarrow K^+K^-)$ decays to a sample of 5.2 fb^{-1} collected by the dimuon trigger [4]. Improvements over the previous version of the analysis include (a) a doubled event sample along with a newly optimized selection (b) a fully data-driven recalibration of the flavor-tagging algorithms (c) inclusion of possible non- ϕ scalar K^+K^- contributions as $B_s^0 \rightarrow J/\psi f_0(980)$.

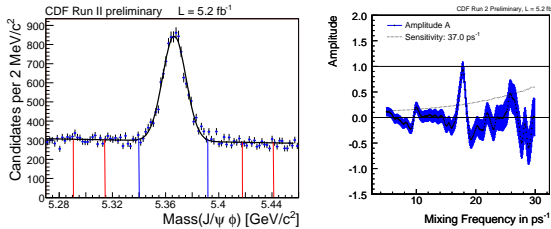


Figure 4. Distribution of $J/\psi K^+ K^-$ mass after the optimized selection.

A kinematic fit to a common space-point is applied to the candidate J/ψ and two tracks consistent with being kaons originated from a ϕ meson decay. A NN trained on simulated data (to identify signal) and B_s^0 mass sidebands (for background) exploits kinematic and PID information for an unbiased optimization of the selection: we minimize the average expected statistical uncertainty on the mixing phase extracted from ensembles of statistical trials generated with different input values. Discriminating observables used include kaon-likelihood, from the combination of dE/dx and TOF information; transverse momenta of the B_s^0 and ϕ mesons; the K^+K^- mass; and the quality of the vertex fit. The final sample contains approximately 6500 signal events over a comparable background (fig. 4, left). The angular distributions of final state particles provide a statistical determination of the CP-composition of the signal thus improving sensi-

tivity to the phase. Possible contributions from scalar $J/\psi K^+ K^-$ or $J/\psi f_0(980)$ final states are included in the angular distributions. The production flavor is inferred using two classes of algorithms. Opposite-side tags (OST) exploit flavor conservation in strong interaction. Being b -quarks predominantly produced in pairs with \bar{b} -quarks, the production flavor is inferred from the charge of decay products (e , μ , or jet) of the b -hadron emitted in the opposite hemisphere of the signal B_s^0 . Same-side tags (SST) exploit flavor conservation in the fragmentation process that leads to the signal B_s^0 meson. Because a $s\bar{s}$ pair will be required to form a meson from the bottom quark, the charge of a kaon kinematically close to the bottom-strange meson is correlated to its flavor. The performance of flavor taggers is modeled as function of many event properties using simulations; however overall scale factors between the simulation and reality are allowed and extracted from data. The uncertainty in their determination contributes to the final systematic uncertainty of the measurement. The tagging power, ϵD^2 , is the product of an efficiency ϵ , the fraction of candidates with a flavor tag, and the square of the dilution $D = 1 - 2w$, where w is the mistag probability. We calibrate independently b and \bar{b} OST tags using 52,000 $B^+ \rightarrow J/\psi K^+$ decays. Predicted and measured dilutions agree with scale factors close to unity. The observed tagging efficiency is $(94.2 \pm 0.4)\%$ and the average predicted dilution on signal is $\sqrt{\langle D^2 \rangle} = 0.110 \pm 0.002$, with 1.03 ± 0.06 scale factor. The SST calibration is obtained by repeating the full mixing analysis on 13,000 $B_s^0 \rightarrow D_s^- \pi^+ (\pi^+ \pi^-)$ [7]. The resulting frequency, $\Delta m_s = 17.79 \pm 0.07 \text{ (stat.) ps}^{-1}$, is fully consistent with published values (fig. 4, right). The scale factor, $A = 0.94 \pm 0.15 \text{ (stat.)} \pm 0.13 \text{ (syst.)}$ is given by the size of the amplitude at the mixing frequency. This corresponds to a tagging efficiency of $(52.2 \pm 0.7)\%$ and an average dilution on signal of $\sqrt{\langle D^2 \rangle} = 0.275 \pm 0.003$. Multiple tags, if any, are combined as independent for a total tagging power $\epsilon D^2 \approx 4.5\%$. The proper time of the decay and its resolution are known on a per-candidate basis with an average resolution of approximately 90 fs^{-1} . Information on B_s^0 candidate mass and its uncertainty, angles

between final state particles' trajectories (to extract the CP-composition), production flavor, and decay length and its resolution are used as observables in a multivariate unbinned likelihood fit of the time evolution that accounts for direct decay amplitude, mixing followed by the decay, and their interference. Direct CP-violation is expected small and neglected. The fit determines the phase $\beta_s^{J/\psi\phi}$, the decay-width difference $\Delta\Gamma$, and many other “nuisance” parameters including the mean B_s^0 lifetime ($2/(\Gamma_L + \Gamma_H)$), the magnitudes of linear polarization amplitudes, the CP-conserving phases ($\delta_{\parallel} = \arg(A_{\parallel}A_0^*)$, $\delta_{\perp} = \arg(A_{\perp}A_0^*)$), and others. The acceptance of the detector is calculated from simulation and found to be consistent with angular distributions of random combinations of four tracks in data; the fit model was validated by measuring lifetime and polarization amplitudes in $B^0 \rightarrow J/\psi K^{*0}$ decays to be consistent with B -factories measurements [9].

For enhanced precision, all parameters but the mixing phase are determined in a fit with phase fixed to zero: $c\tau(B_s^0) = 458.6 \pm 7.6$ (*stat.*) ± 3.6 (*syst.*) μm , $\Delta\Gamma = 0.075 \pm 0.035$ (*stat.*) ± 0.010 (*syst.*) ps^{-1} , $|A_{\parallel}|^2 = 0.231 \pm 0.014$ (*stat.*) ± 0.015 (*syst.*), $|A_0|^2 = 0.524 \pm 0.013$ (*stat.*) ± 0.015 (*syst.*), and $\delta_{\perp} = 2.95 \pm 0.64$ (*stat.*) ± 0.07 (*syst.*) rad. These results represent the current best measurements of these quantities from a single experiment.

With phase floating, fits on simulated samples show biased, non-Gaussian distributions of estimates and multiple maxima, because of known likelihood symmetries. We use a frequentist confidence region in the $(\beta_s^{J/\psi\phi}, \Delta\Gamma)$ plane using a profile-likelihood ratio ordering [10], which is close to optimal for limiting the impact of systematic uncertainties. These are included by randomly sampling a limited number of points in the space of all nuisance parameters. A specific value $(\beta_s^{J/\psi\phi}, \Delta\Gamma)$ is excluded only if it can be excluded for any assumed value of the nuisance parameters within 5σ of their estimate on data.

The resulting allowed region is greatly reduced with respect to the previous measurement and is fairly consistent (0.8σ) with the SM: the range $[0.02, 0.52] \cup [1.08, 1.55]$ contains the $\beta_s^{J/\psi\phi}$ phase

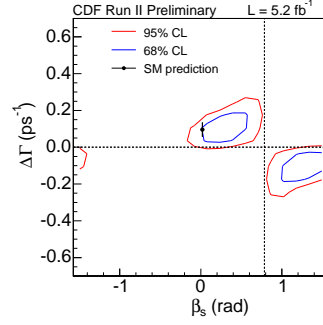


Figure 5. Confidence region in the $(\beta_s^{J/\psi\phi}, \Delta\Gamma)$ plane.

at the 68% CL and the range $[-\pi/2, -1.44] \cup [-0.13, 0.68] \cup [0.89, \pi/2]$ at the 95% CL.

With the full Run II data sample, we expect to observe a non-SM phase or exclude it for any value of $\beta_s^{J/\psi\phi}$ larger than approximately 0.4 rad.

REFERENCES

1. CDF Collaboration, Note 10064, and D. Acosta *et al.* (CDF Collaboration), Phys. Rev. Lett. 95, 031801 (2005).
2. Heavy Flavor Averaging Group, arXiv:[1010.1589(hep-ex)].
3. CDF Collaboration, Note 10120.
4. CDF Collaboration, Note 10206, and T. Aaltonen *et al.* (CDF Collaboration), Phys. Rev. Lett. 100, 161802 (2008).
5. CDF Collaboration, Note 9892, and T. Aaltonen *et al.* (CDF Collaboration), Phys. Rev. Lett. 100, 101802 (2008).
6. CDF Collaboration, Note 10047, and T. Aaltonen *et al.* (CDF Collaboration), Phys. Rev. D79, 011104(R) (2009).
7. CDF Collaboration, Note 10108, and A. Abulencia *et al.* (CDF Collaboration), Phys. Rev. Lett. 97, 242003 (2006).
8. U. Nierste, talk at CKM Workshop 2010.
9. CDF Collaboration, Note 8950.
10. D. Tonelli (for the CDF Collaboration), arXiv:[0810.3229(hep-ex)].